Temperature Dependence of Proton NMR Chemical Shift As a Criterion To Identify Low-Barrier Hydrogen Bonds

Mireia Garcia-Viloca, Ricard Gelabert, Àngels González-Lafont, Miquel Moreno, and José M. Lluch*

Contribution from the Departament de Química, Universitat Autònoma de Barcelona, 08193 Bellaterra (Barcelona), Spain

Received December 12, 1997. Revised Manuscript Received June 29, 1998

Abstract: The NMR chemical shifts of the proton participating in the intramolecular hydrogen bond in a realistic model of hexabenzyloxymethyl-XDK [*m*-xylidenediamine-bis(Kemp's triacid)-imide] monoanion and hydrogen oxalate anion have been theoretically analyzed. Ab initio and density functional theory (DFT) calculations are fitted to a monodimensional potential energy surface where the nuclear Schrödinger equation can be solved to obtain the vibrational levels and their corresponding wave functions. Our results indicate that for hexabenzyloxymethyl-XDK monoanion, the first vibrational level appears above the transition state, and the ground vibrational state wave function has a maximum value just at the transition state region so that, as observed experimentally, the hexabenzyloxymethyl-XDK monoanion has a low-barrier hydrogen bond. Conversely, for the hydrogen oxalate anion, the ground vibrational level is well below the energy barrier separating the two minima so that the proton is most probably found at or near the minima and the hydrogen bond is of the "normal" type. We have also analyzed the effect of temperature on the chemical shift by performing Boltzmann averages along the vibrational states in each case. We have found that for hexabenzyloxymethyl-XDK monoanion the chemical shift decreases as the temperatures increases whereas the reverse trend is observed for the hydrogen oxalate anion. Therefore the presence of a negative slope of the chemical shift as a function of the temperature could be used to characterize a hydrogen bond in a symmetric potential as a low-barrier hydrogen bond in gas phase and possibly in inert solvents.

Introduction

Interest in the nature of low-barrier hydrogen bonds (LBHBs),[1] also known as Speakman−Hadzi hydrogen bonds,[2] has recently revived because of the presumed role of these bonds during enzyme catalysis.[3−15] The magnitude of the energetics of those LBHBs is nowadays a question open to discussion among experimentalists and theoreticians working in different fields where Speakman−Hadzi hydrogen bonds have been detected.[16−27]

Recently, Kato et al.[28] experimentally measured the strength of an LBHB in nonpolar solvents, using synthetic molecules derived from *m*-xylidenediamine-bis(Kemp's triacid)-imide (XDK). In particular, the highly lipophilic hexabenzyloxymethyl-XDK diacid (Scheme 1) was synthesized for study in apolar media. XDK, as well as the synthesized derivative of Scheme 1, presents two unconjugated acids, rigidly locked into a conformation that enforces the formation of two intramolecular hydrogen bonds. Kato et al. indicated that the large second pK_a of XDK in aqueous solution, which was attributed to the repulsion of two negative charges at a small distance in the dianion, might also be explained by the formation of a strong LBHB in the XDK monoanion. However, because the existence of LBHBs in aqueous solution has been the source of some debate,[13,17,22,26,29] Kato et al. carried out their experiments in apolar organic media. The measured ^{1}H NMR spectra at 25

* To whom correspondence should be addressed. Tel: 34-93-581-2138. Fax: 34-93-581-2920. E-mail: lluch@klingon.uab.es.

(1) Cleland, W. W. *Biochemistry* **1992**, *31*, 317.
(2) (a) Speakman, J. C. *J. Chem. Soc.* **1949**, 3357. (b) Hadzi, D. *Pure Appl. Chem.* **1965**, *11*, 435. (c) Gerlt, J. A.; Kreevoy, M. M.; Cleland, W. W.; Frey, P. A. *Chem. Biol.* **1997**, *4*, 259.
(3) Gerlt, J. A.; Gassman, P. G. *J. Am. Chem. Soc.* **1993**, *115*, 11552.
(4) Gerlt, J. A.; Gassman, P. G. *Biochemistry* **1993**, *32*, 11943.
(5) Cleland, W. W.; Kreevoy, M. M. *Science* **1994**, *264*, 1887.
(6) Frey, P. A.; Whitt, S. A.; Tobin, J. B. *Science* **1994**, *264*, 1927.
(7) Kenyon, G. L.; Gerlt, J. A.; Petsko, G. A.; Kozarich, J. W. *Acc. Chem. Res.* **1995**, *28*, 178.
(8) Tong, H.; Davis, L. *Biochemistry* **1995**, *34*, 3362.
(9) Xiang, S.; Short, S. A.; Wolfenden, R.; Carter, C. W. *Biochemistry* **1995**, *34*, 4516.
(10) Hur, O.; Leja, C.; Dunn, M. F. **1996**, *35*, 7378.
(11) Cleland, W. W.; Kreevoy, M. M. *Science* **1995**, *269*, 104.
(12) Frey, P. A. *Science* **1995**, *269*, 104.
(13) Zhao, Q.; Abeygunawardana, C.; Talalay, P.; Mildvan, A. S. *Proc. Natl. Acad. Sci. U.S.A.* **1996**, *93*, 8220.
(14) Cassidy, C. S.; Lin, J.; Frey, P. A. *Biochemistry* **1997**, *36*, 4576.
(15) Kahyaoglu, A.; Haghjoo, K.; Guo, F.; Jordan, F.; Kettner, C.; Felföldi, F.; Polgár, L. *J. Biol. Chem.* **1997**, *272*, 25547.
(16) Usher, K. C.; Remington, S. J.; Martin, D. P.; Drueckhammer, D. G. *Biochemistry* **1994**, *33*, 7753.
(17) Warshel, A.; Papazyan, A.; Kollman, P. A. *Science* **1995**, *269*, 102.
(18) Schwartz, B.; Drueckhammer, D. G. *J. Am. Chem. Soc.* **1995**, *117*, 11902.
(19) Scheiner, S.; Kar, T. *J. Am. Chem. Soc.* **1995**, *117*, 6970.
(20) Warshel, A.; Papazyan, A. *Proc. Natl. Acad. Sci. U.S.A.* **1996**, *93*, 13665.
(21) Shan, S.-O.; Herschlag, D. *Proc. Natl. Acad. Sci. U.S.A.* **1996**, *93*, 14474.
(22) Guthrie, J. P. *Chem. Biol.* **1996**, *3*, 164.
(23) Garcia-Viloca, M.; González-Lafont, A.; Lluch, J. M. *J. Am. Chem. Soc.* **1997**, *119*, 1081.
(24) Garcia-Viloca, M.; González-Lafont, A.; Lluch, J. M. *J. Phys. Chem.* **1997**, *101*, 3880.
(25) Ash, E. L.; Sudmeier, J. L.; De Fabo, E. C.; Bachovchin, W. W. *Science* **1997**, *278*, 1128.
(26) Pan, Y.; McAllister, M. A. *J. Am. Chem. Soc.* **1997**, *119*, 7561.
(27) McAllister, M. A. *Can. J. Chem.* **1997**, *75*, 1195.
(28) Kato, Y.; Toledo, L. M.; Rebek, J., Jr. *J. Am. Chem. Soc.* **1996**, *118*, 8575.

S0002-7863(97)04214-5 CCC: $15.00 © 1998 American Chemical Society
Published on Web 09/19/1998

Scheme 1

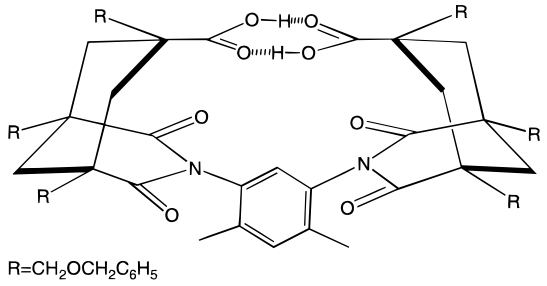

°C for the hexabenzyloxymethyl-XDK diacid presents a signal at 12.6 ppm. When triethylamine is added to the solution, the ^{1}H NMR signal for the formed monoanion moves downfield to 18 ppm, a value that, according to Kato et al., is consistent with the existence of an LBHB in the system. At this point, we should recall that, as has been previously shown, an unusually downfield chemical shift (δ) does not necessarily imply the formation of an LBHB.[20,22,30] Our opinion is that the only requirement for a hydrogen bond to be characterized by a downfield chemical shift is that it must be short at the minimum energy structures of the proton transfer along the hydrogen bond. However, because the short acceptor−donor distance is also a requirement for LBHB formation, those two features (high chemical shifts and LBHB character) may usually come together.[30] Although other definitions[3,14,26,31,32] of an LBHB have been based on its strength, in this work, as well as in the paper mentioned above, we will use an operational definition of an LBHB that does not go beyond what is already implied in the name "low-barrier hydrogen bond." In a monodimensional approach, a hydrogen bond can be defined as an LBHB if the ground vibrational level of the monodimensional double well lies at or above the classical energy barrier (i.e., without including zero point energy) for the proton transfer, according to the definition given by Cleland and Kreevoy.[5] More generally, we assume that an LBHB appears when the classical energy barrier for the proton transfer along the hydrogen bond is low enough so that the double well ground vibrational wave function reaches its maximum values at the region of that energy barrier. The first objective of our work will consist of verifying, by quantum mechanical calculations in gas phase, whether or not the intramolecular hydrogen bond in hexabenzyloxymethyl-XDK monoanion turns out to be an LBHB in accordance with the above-mentioned definition.

Kato et al. also reported interesting experimental data showing how the ^{1}H NMR chemical shift of the participating proton of a symmetric $(O\cdots H\cdots O)^-$ LBHB depends on temperature. Concretely, they observed that the downfield NMR resonance signal at 25 °C moved even further downfield (to 19.2 ppm) when the hexabenzyloxymethyl-XDK monoanion was cooled to −70 °C.[28]

The second and main objective of the present work is to study theoretically and understand the temperature dependence of the ^{1}H NMR chemical shift associated with the participating hydrogen in an LBHB. To this aim, we have designed a model (structure **1** in Scheme 2) to evaluate the chemical shift in hexabenzyloxymethyl-XDK monoanion. However, as we are interested in comparing our theoretical results with experimental chemical shift measurements, we will need to evaluate chemical

Scheme 2

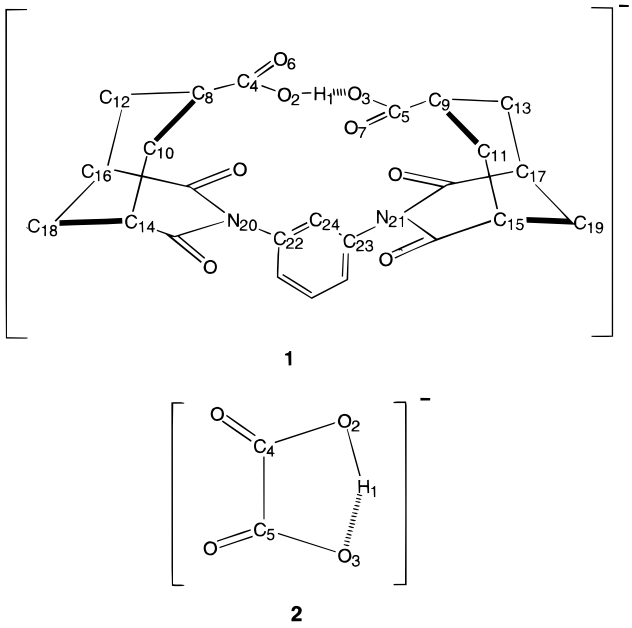

1

2

shifts values corresponding to a vibrational state rather than to a frozen arrangement of nuclei. Concretely, this implies evaluating an averaged δ value, $\langle\delta\rangle_i$, using the probability density function of the vibrational state i, as a weighting factor. Finally, $\langle\delta\rangle_T$ values as a function of temperature will be calculated to compare our findings with the experimental trends associated with LBHB behavior. For comparison, we will also calculate the temperature dependence of the ^{1}H NMR chemical shift of the participating proton in the intramolecular hydrogen bond of hydrogen oxalate (structure **2** in Scheme 2), a non-LBHB.[30]

Calculation Details

Two different models have been used to study the intramolecular hydrogen bond in hexabenzyloxymethyl-XDK monoanion. The first model is displayed in Scheme 2 (**1**) and corresponds to the monoanion of the diacid in Scheme 1 with R═H and with the methyl groups of the benzene replaced by hydrogens. Despite these changes, the number of atoms of model **1** is as many as 57. Full geometry optimization and direct localization of stationary points, minima or transition-state structures of the proton transfer, have been done at both the PM3[33] semiempirical and the ab initio Hartree−Fock (HF) levels of calculation. Both kinds of stationary points, minima or transition-state structures, have been characterized by diagonalizing their Hessian matrixes and looking for zero or one negative eigenvalue, respectively. The HF calculations have been carried out by using the split valence 6-31G basis set,[34] which implies 352 basis functions for model **1**. We will refer to the 6-31G basis set as b1. To introduce the electron correlation, single-point energy calculations have been done by using the density functional theory (DFT)[35] on the HF-optimized geometries. Concretely, the three-parameter hybrid functional of Becke and the Lee, Yang, and Parr's correlation functional, widely known as Becke3LYP, has been used.[36] As recently shown, DFT methods should be reliable for the study of LBHB systems.[26] In those single-point calculations, the basis

(29) Perrin, C. L. *Science* **1994**, *266*, 1665.
(30) Garcia-Viloca, M.; Gelabert, R.; González-Lafont, A.; Moreno, M.; Lluch, J. M. *J. Phys. Chem. A* **1997**, *101*, 8727.
(31) Shan, S.-O.; Loh, S.; Herschlag, D. *Science* **1996**, *272*, 97.
(32) Shan, S.-O.; Herschlag, D. *J. Am. Chem. Soc.* **1996**, *118*, 5515.
(33) Stewart, J. J. P. *J. Comput. Chem.* **1989**, *10*, 209.
(34) Ditchfield, R.; Hehre, W. J.; Pople, J. A. *J. Chem. Phys.* **1971**, *54*, 724.
(35) (a) Kohn, W.; Becke, A. D.; Parr, R. G. *J. Phys. Chem.* **1996**, *100*, 12974. (b) Parr, R. G.; Yang, W. *Density Functional Theory of Atoms and Molecules*; Oxford University Press: New York, 1989. (c) Dreizler, R. M.; Gross, E. K. V. *Density Functional Theory*; Springer: Berlin, 1990.
(36) (a) Becke, A. D. *J. Chem. Phys.* **1993**, *98*, 5648. (b) Becke, A. D. *J. Chem. Phys.* **1996**, *104*, 1040. (c) Becke, A. D. In *Modern Electronic Structure Theory*; Yarkony, D.R., Ed.; World Scientific: Singapore, 1995.

Scheme 3

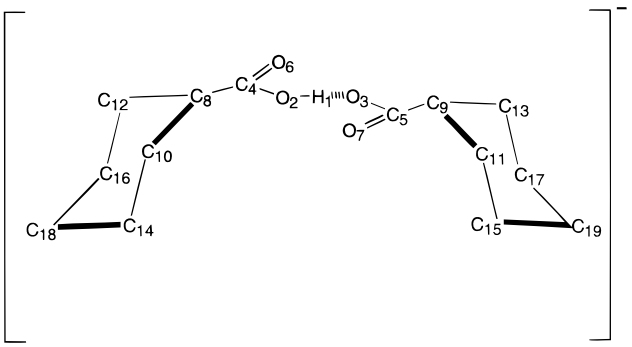

3

set used is the split-valence 6-31G, except for the atoms that form the hydrogen bond and their nearest neighbors, that is: H_1, O_2, O_3, C_4, C_5, O_6, and O_7 in Scheme 2 (**1**), where we have added a *d* or a *p* polarization function on heavy or hydrogen atoms, respectively, and a diffuse *sp* shell on heavy atoms.[37] In other words, we have used a mixed basis set, made of the 6-31G basis set for most of the atoms and the 6-31+G(d,p) basis set for the atoms related to the hydrogen bond. We will refer to this mixed basis set as b2. The basis set b2 used in the calculations of model **1** sums up 409 basis set functions, what explains why the DFT/b2 optimization of the geometry of **1** is beyond our calculation capabilities.

The second model of the hexabenzyloxymethyl-XDK monoanion is represented in Scheme 3 (**3**). In this model the number of atoms is reduced to 41 because we have removed the part of the system that does not significantly move along the intramolecular proton transfer. This model has been built from the PM3-optimized geometry of the first model (**1**), keeping fixed the Cartesian coordinates of six carbon atoms C_{16}, C_{18}, C_{14}, C_{15}, C_{17}, and C_{19}. Maintaining this constraint, we have optimized the minimum energy structure of **3** both at the PM3 semiempirical level and the HF and DFT levels of calculation, using the b2 basis set. Using the b2 basis set in the calculations of **3** involves 265 basis functions.

In the study of the intramolecular hydrogen bond in hydrogen oxalate (**2**), full geometry optimization and direct localization of stationary points have been done at the second-order Møller−Plesset perturbation theory[38,39] (MP2) by using the split-valence 6-31+G(d,p) basis set. The Hessian matrixes of the stationary points have been calculated to characterize both kinds of stationary points, minima and transition-state structures.

^{1}H NMR chemical shifts (δ) relative to hydrogen atoms in $Si(CH_3)_4$ were obtained from nuclear magnetic shielding tensors calculated through the gauge invariant atomic orbital (GIAO)[40,41] method. The GIAO chemical shifts have been calculated by using the DFT wave function with the split-valence 6-31+G(d,p) basis set in the case of hydrogen oxalate, and the mixed b2 basis set in the model of the XDK monoanion (**1**). The use of this locally dense (mixed) basis set should be suitable in light of suggestions that the determination of the chemical shift for a particular atom depends mainly on the local basis set, and less on whether a balanced or unbalanced (mixed) calculation is being performed.[42] All electronic structure calculations have been done with the GAUSSIAN 94 package.[43]

We are interested in evaluating the values of the chemical shifts of transferring protons that correspond to a given vibrational state rather than to a frozen arrangement of nuclei (that is, a fixed molecular geometry). Concretely, this implies evaluating averaged chemical shifts by using $|\Psi|^2$, the square of the vibrational wave function, as a weighting factor. Consequently, we have to obtain the vibrational eigenvalues and eigenfunctions. To do so, the nuclear motion Schrödinger equation has to be solved:

$$[\hat{T}_{nuc} + U(\boldsymbol{R})]\Psi = E\Psi \tag{1}$$

where U(**R**) is the complete potential energy hypersurface, which depends on **R**, a 3N−6 dimension vector that describes each different geometrical arrangement of the atoms of the molecule. Of course, calculating the whole U(**R**) is impossible except for the simplest of all systems, so a drastic simplification is needed. The most straightforward simplification consists of reducing the dimensionality of U(**R**) to just one dimension. In this way, both the evaluation of U and solving eq 1 become feasible tasks for sizable systems. The problem is choosing the variable on which U depends. Given that any monodimensional path is just as good as any other, provided it represents the chemical process under study (in our case, an intramolecular proton transfer within the corresponding hydrogen bond), we have opted for a linear interpolation in mass-weighted Cartesian coordinates linking the transition state structure with the reactants' structure and then we extrapolate beyond that point farther from reactants; then we make yet another linear interpolation in the same coordinate system going from the transition state structure to the products' minimum and again make the corresponding extrapolation beyond. These linear paths have been constructed by orienting both structures involved in such a way that neither linear nor angular momenta were generated when going from one to the other.[44] After the number of variables of U has been reduced in this way to just 1, we use a basis set methodology to solve eq 1.[45] Within this methodology, the vibrational energy levels and wave functions are obtained through diagonalization of the matrix representation of the Hamiltonian operator in eq 1, projected over a basis set made up of monodimensional Gaussian functions:

$$\chi_j(s) = \left(\frac{\alpha}{\pi}\right)^{1/4} \exp\left[-\frac{\alpha}{2}(s - s_j)^2\right] \tag{2}$$

where *s* is the arc distance along the reaction path in mass-weighted Cartesian coordinates, and $\{s_j\}$ is the set of equally spaced points along the aforementioned linear paths. In this way *n* variational approximations to the lowest *n* eigenvalues and eigenfunctions can be obtained by using *n* basis functions. In this work, different numbers of basis functions were used in the different cases, so that the density of Gaussian functions was approximately the same in the two systems studied. We also checked that a further increase in the number of basis functions did not noticeably change the position of the vibrational levels (results not shown).

The vibrational wave function so obtained is expressed as a linear combination of basis functions. To account for motions of the nuclei in a vibrational state, δ values of the proton have been evaluated at several points along the path (*s*), and then fitted into a cubic spline functional form. Finally, the mean value of δ is obtained as an average all over the vibrational state *i* by taking into account the appropriate probability density function, in this case $|\Psi_i|^2$, by means of:

$$\langle\delta\rangle_i = \frac{\int_{-\infty}^{+\infty} \Psi_i(s)\, \delta(s)\, \Psi_i(s)\, \mathrm{d}s}{\int_{-\infty}^{+\infty} \Psi_i(s)\, \Psi_i(s)\, \mathrm{d}s} \tag{3}$$

(37) (a) Clark, T.; Chandrasekhar, J.; Spitznagel, G. W.; Schleyer, P.v. R. *J. Comput. Chem.* **1983**, *4*, 294. (b) Frisch, M. J.; Pople, J. A.; Binkley, J. S. *J. Chem. Phys.* **1984**, *80*, 3265.

(38) Møller, C.; Plesset, M. S. *Phys. Rev.* **1934**, *46*, 618.

(39) Binkley, J. S.; Pople, J. A. *Int. J. Quantum Chem.* **1975**, *9*, 229.

(40) Ditchfield, R. *Mol. Phys.* **1974**, *27*, 789.

(41) Wolinski, K.; Hinton, J. P.; Pulay, P. *J. Am. Chem. Soc.* **1990**, *112*, 8251.

(42) Chesnut, D. B.; Moore, K. D. *J. Comput. Chem.* **1989**, *10*, 648.

(43) Frisch, M. J.; Trucks, G. W.; Schlegel, H. B.; Gill, P. M. W.; Johnson, B. G.; Robb, M. A.; Cheeseman, J. R.; Keith, T. A.; Petersson, G. A.; Montgomery, J. A.; Raghavachari, K.; Al-Laham, M. A.; Zakrzewski, V. G.; Ortiz, J. V.; Foresman, J. B.; Cioslowski, J.; Stefanov, B. B.; Nanayakkara, A.; Challacombe, M.; Peng, C. Y.; Ayala, P. Y.; Chen, W.; Wong, M. W.; Andres, J. L.; Replogle, E. S.; Gomperts, R.; Martin, R. L.; Fox, D. J.; Binkley, J. S.; Defrees, D. J.; Baker, J.; Stewart, J. P.; Head-Gordon, M.; Gonzalez, C.; Pople, J. A. *Gaussian94*; Gaussian: Pittsburgh, PA, 1995.

Table 1. Main Geometric Parameters of the Minimum Energy Structure and the Transition State (TS) for the Intramolecular Proton Transfer Corresponding to System **1** (see Scheme 2)

	minimum energy structure			TS,
	PM3	HF/b1	DFT/b2	DFT/b2
	Distances, Å			
O_2-H_1	0.98	1.04	1.13	1.19
H_1-O_3	1.71	1.44	1.29	1.19
O_2-O_3	2.62	2.48	2.42	2.39[a]
O_6-O_7	4.46	5.34	5.34	5.34
C_4-C_5	4.35	4.44	4.41	4.39
	Angles, deg			
$O_2-H_1-O_3$	153.1	177.1	177.2	177.6
$C_4-H_1-C_5$	163.2	165.4	168.6	170.1
$C_{14}-C_{10}-C_8$	116.85	114.91	115.01	115.07
$N_{20}-C_{22}-C_{24}$	120.96	119.56	119.35	119.22
$N_{21}-C_{23}-C_{24}$	119.67	119.18	119.23	119.26
$C_{15}-C_{11}-C_9$	116.10	114.17	114.17	114.16
$O_6-C_4-O_2-H_1$	−9.0	−5.3	−2.9	−1.4
$O_7-C_5-O_3-H_1$	10.3	2.3	−0.4	−2.3
$C_{10}-C_8-C_4-O_6$	−161.0	155.5	159.1	161.4
$C_{13}-C_9-C_5-O_7$	−159.1	166.03	164.82	164.06

[a] As a consequence of a numerical rounding effect, the O_2-O_3 distance exceeds the sum of the O_2-H_1 and H_1-O_3 distances.

Finally, a Boltzmann average weighting each $\langle\delta\rangle_i$ according to the thermal equilibrium population of each vibrational state i has been performed to obtain $\langle\delta\rangle_T$.

Results and Discussion

As indicated in the Introduction this paper is aimed at the comparative study of the behavior of proton NMR chemical shift in hexabenzyloxymethyl-XDK monoanion and in hydrogen oxalate as a function of temperature. The first molecule is thought to involve an LBHB. The second is known to contain a normal hydrogen bond, in the sense that the proton is localized in the neighborhood of one oxygen, either the donor or the acceptor.

Because the hexabenzyloxymethyl-XDK monoanion is quite large (57 atoms), we have focused on the somewhat simpler system **1** (see Scheme 2), which we have since reduced to system **3** shown in Scheme 3 (still containing 41 atoms) as a reduced model of **1**.

First of all, the minimum energy structure of **1** has been located at the PM3 level of calculation. From this geometry, and following the procedure outlined above, we have built up the constrained molecule **3**, which we have also optimized at the PM3 level. However, a comparison between the two PM3 structures shows important differences (see Tables 1 and 2). Thus, the distance between the C_4 and the C_5 atoms and the angle for $C_4-H_1-C_5$ in **3** are both quite smaller than in **1**. More importantly, the $C_{10}-C_8-C_4-O_6$ and $C_{13}-C_9-C_5-O_7$ dihedral angles are alike in **1** but differ considerably in **3**. This dissimilarity is a consequence of a rotation of the $C_{13}-C_9-C_5-O_7$ dihedral angle in **3** that shortens very noticeably the O_6O_7 distance in comparison with the distance in structure **1**. Reoptimization of system **3** at the HF and DFT levels using the b2 basis set (see Table 2) leads to geometries that show the same trends of the PM3 minimum energy structure of that system (apart from some changes in the parameters directly involved in the hydrogen bond). On the other hand, an HF reoptimization of system **1** using the b1 basis set gives rise to a geometry (Table 1) that retains the main features of the corresponding PM3 structure (putting aside some changes in the parameters directly involved in the hydrogen bond). Thus it is unfortunately clear that system **3** is not a suitable model of system **1**. As a consequence, we are forced to treat system **1** (henceforth called the XDK model) without additional reduction, although this limits the calculation level we are able to use to solve the electronic Schrödinger equation. However, it is known that electron correlation significantly modifies the energetic and geometric parameters associated with hydrogen bonds. These changes are already seen in Table 2 when comparing the HF and DFT minimum energy structures of system **3**. As expected, electron correlation shortens the donor oxygen−acceptor oxygen ($O_2\cdots O_3$) distance and the hydrogen−acceptor oxygen ($H_1\cdots O_3$) distance in the hydrogen bond, while it lengthens the donor oxygen−hydrogen ($O_2\cdots H_1$) distance.

Table 2. Main Geometric Parameters of the Minimum Energy Structure Corresponding to System **3** (see Scheme 3)

	minimum energy structure		
	PM3	HF/b2	DFT/b2
	Distances, Å		
O_2-H_1	0.99	1.01	1.17
H_1-O_3	1.69	1.51	1.26
O_2-O_3	2.66	2.52	2.42
O_6-O_7	4.00	4.14	4.00
C_4-C_5	4.07	3.98	3.90
	Angles, Å		
$O_2-H_1-O_3$	168.5	174.8	173.0
$C_4-H_1-C_5$	137.4	133.4	132.3
$C_{14}-C_{10}-C_8$	114.3	114.0	113.1
$C_{15}-C_{11}-C_9$	111.5	111.4	111.8
$O_6-C_4-O_2-H_1$	5.3	1.0	0.0
$O_7-C_5-O_3-H_1$	26.3	28.9	23.1
$C_{10}-C_8-C_4-O_6$	−121.2	−93.9	−81.7
$C_{13}-C_9-C_5-O_7$	170.6	146.8	140.3

To introduce in our calculations of system **1** some degree of electron correlation, we applied the following strategy. First of all, we located the transition state for the intramolecular proton transfer along the hydrogen bond of molecule **1** at the HF/b1 level of calculation. Then we performed a linear interpolation between each HF/b1 minimum (since the proton transfer is symmetric, the two minima are equivalent) and the HF/b1 transition state, thus generating a series of points with geometries intermediate between the two minima and passing through the transition state. By performing single-point DFT/b2 calculations at every point along such a path we obtained a monodimensional energy profile, whose minima and maxima are, respectively, the DFT/b2 minimum energy structures and transition state (Table 1) for the proton transfer. This procedure is more expensive but more reliable than the simple energy recalculation at some higher level while keeping frozen the geometries of the stationary points located at a lower level of electronic calculations.[46] By doing this, the DFT results yield a classical potential energy curve for proton transfer involving two minima, geometrically much closer that the two HF minima (the same scenario as the one previously described for system **3**), separated by a transition state. The classical energy barrier turns out to be only 0.06 kcal/mol, a vanishingly small value. On the other hand, the arrangement of the two carboxylate groups sharing the proton at the minimum energy structure corresponds to a so-called *syn-syn* hydrogen bond.[28] From here on all the results referring to the XDK model will correspond to the DFT/b2 calculations.

(44) Miller, W. H.; Ruf, B. A.; Chang, Y. *J. Chem. Phys.* **1988**, *89*, 6298.

(45) (a) Hamilton, I. P.; Light, J. *J. Chem. Phys.* **1986**, *84*, 306. (b) Makri, N.; Miller, W. H. *J. Chem. Phys.* **1987**, *86*, 1451.

(46) Paz, J. J.; Moreno, M.; Lluch, J. M. *J. Chem. Phys.* **1997**, *107*, 6275.

Table 3. Main Geometrical Parameters of Hydrogen Oxalate Minimum Energy Structure and the Corresponding Transition State (TS) for the Intramolecular Proton Transfer

	minimum energy structure	TS
	Distances, Å	
O_2-H_1	1.00	1.22
H_1-O_3	1.71	1.22
O_2-O_3	2.50	2.33
	Angles, deg	
$O_2-H_1-O_3$	132.1	144.6
$C_4-O_2-H_1$	99.0	91.0
$C_5-O_3-H_1$	88.2	91.0
$O_3-C_5-C_4-O_2$	0.0	0.0

Table 4. Proton NMR Chemical Shifts (ppm) for the Minimum Energy Structures and Transition States of the XDK Model and Hydrogen Oxalate

	XDK model	hydrogen oxalate
minimum	21.07	13.28
TS	21.71	21.69

As for hydrogen oxalate **2**, the main MP2 geometrical parameters of the minimum energy structure and transition state for the intramolecular proton transfer are given in Table 3. The corresponding classical energy barrier was calculated to be 3.12 kcal/mol.[30]

Let us now consider the ^{1}H NMR chemical shift corresponding to the transferring proton. δ values for the minimum energy structures and transition states of the XDK model and hydrogen oxalate, given in Table 4, follow the trends already shown in previous works.[30,47,48] The proton chemical shift in the O−H···O hydrogen bond is enhanced as the O−H distance increases and also as the O···O distance (or rather, the H···O distance) decreases. In consequence (see the hydrogen bond distances in Tables 1 and 3) the transition states exhibit a very low-field proton signal (a very high δ value) because the shifting proton lies at the midpoint region between both heavy atoms (large O−H distance, but relatively short H···O distance, specially taking into account that the O···O distance tends to diminish when going from the minimum to the transition state). Minimum energy structures behave in a different way. If the hydrogen bond is short enough (as in the XDK model), the O−H distance tends to be large and the H···O distance rather short, leading to a very deshielded proton (almost as much as in the transition state). Otherwise (as for hydrogen oxalate), the minimum possesses a normal δ value.

Each particular frozen position of the proton has an associated δ value (as in the minimum energy and the transition state structures, which are fixed structures without any nuclear kinetic energy). However, the proton is a quantum particle and, as a consequence, is really delocalized along the potential energy double well corresponding to the hydrogen bond. Several quantum vibrational states associated with the proton motion exist in the double well. Each vibrational state is characterized by its vibrational wave function, which determines the probability density function $|\Psi|^2$ for finding the system (and the proton) at a given position along the double well. An averaged chemical shift $\langle\delta\rangle_i$ over all possible positions in the hydrogen bond, weighted by $|\Psi_i|^2$, would be observed when the system was in a particular vibrational state i. The chemical shift $\langle\delta\rangle_T$ actually "seen" in the NMR experiment at a given temperature T is the Boltzmann-weighted average of $\langle\delta\rangle_i$ over all the vibrational states.

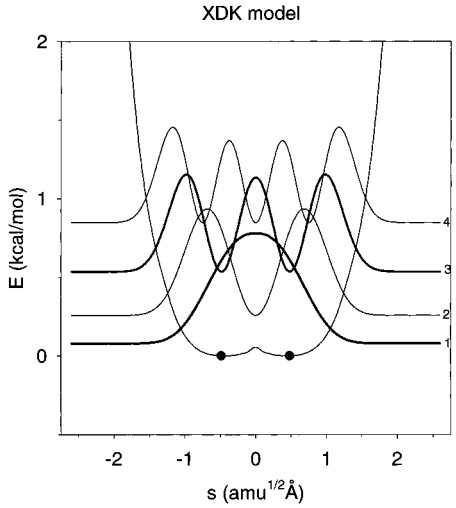

Figure 1. Monodimensional potential energy profile as a function of s (arc distance along the reaction path in mass-weighted Cartesian coordinates) for the XDK model and probability density functions $|\Psi_i|^2$ for the four lowest vibrational states. The horizontal asymptotes of each $|\Psi_i|^2$ curve lie just on the energy level (see y-axis) corresponding to the vibrational state i (indicated on the right). Solid circles indicate the location corresponding to the minimum energy structures.

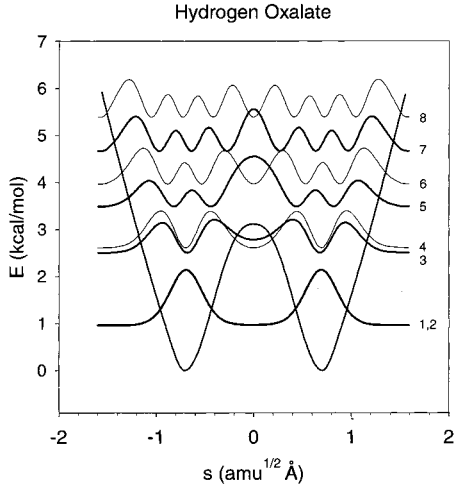

Figure 2. Monodimensional potential energy profile as a function of s (arc distance along the reaction path in mass-weighted Cartesian coordinates) for hydrogen oxalate and probability density functions $|\Psi_i|^2$ for the eight lowest vibrational states. The horizontal asymptotes of each $|\Psi_i|^2$ curve lie just on the energy level (see y-axis) corresponding to the vibrational state i (indicated on the right).

To determine the vibrational states, we followed the procedure outlined in the calculation details section. We chose a monodimensional path consisting of two linear segments as the proton-transfer reaction path. For each system, the potential energy U (DFT and MP2 levels for **1** and **2**, respectively) and the δ values were calculated at several points along the corresponding proton-transfer reaction path. Both magnitudes were fitted into cubic splines functional forms. Then the vibrational wave functions and the energy levels, along with the corresponding $\langle\delta\rangle_i$ values, were calculated for the XDK model and hydrogen oxalate. Results are displayed in Figures 1 and 2 and in Table 5.

Let us first analyze the XDK model. Despite the very small energy barrier for the intramolecular proton transfer, the classical potential energy curve associated with the hydrogen bond has

(47) Ditchfield, R. *J. Chem. Phys.* **1976**, *65*, 3123.
(48) Berglund, B.; Vanghan, R.W. *J. Chem. Phys.* **1980**, *73*, 2037.

Table 5. Energies (E)in kcal/mol and Proton NMR Chemical Shifts ($\langle\delta\rangle_i$) in ppm Corresponding to Different Vibrational States for the XDK Model and Hydrogen Oxalate

vibrational states	XDK model		hydrogen oxalate	
	E	$\langle\delta\rangle_i$	E	$\langle\delta\rangle_i$
1	0.079	21.04	0.964	13.67
2	0.258	20.25	0.969	13.61
3	0.536	19.88	2.506	15.15
4	0.848	19.47	2.613	13.84
5	1.202	19.13	3.489	16.06
6	1.581	18.84	3.967	13.68
7	1.996	18.61	4.665	13.89
8	2.442	18.41	5.389	13.23
9	2.923	18.22		
10	3.428	18.02		
11	3.961	17.82		
12	4.516	17.64		
13	5.097	17.46		

a double well shape with two extremely shallow minima on both sides of the transition state. However, the ground vibrational state appears slightly above the energy barrier, and $|\Psi_1|^2$ reaches its maximum value right at the transition state region. Then the hydrogen bond in the XDK model (and therefore in hexabenzyloxymethyl-XDK monoanion) turns out to be an LBHB, thus confirming the experimental assumptions.[28] The proton is essentially centralized but the nuclear wave function spreads a lot toward both minima and beyond, where the proton is pushed toward the oxygen to which it is bonded, causing a fall of δ. As a consequence, the chemical shift $\langle\delta\rangle_1$ is very high but is smaller than the values corresponding to both the frozen minima and the transition state structures. Note that, as explained in a previous paper, the short oxygen−oxygen distance in the hydrogen bond at the minima causes both the high ^{1}H NMR chemical shift and the existence of an LBHB.[30] However, the extremely low-field proton signal is not in this case a direct consequence of the LBHB because the minimum energy structures themselves already had very high δ values. When going to upper vibrational states, the probability density function moves more and more away from the central region corresponding to the proton-transfer transition state, and becomes more and more important outside the region between the two minima. As a consequence, as seen in Table 5, the higher the vibrational state, the smaller the proton chemical shift associated with it.

The scenario for hydrogen oxalate is entirely different. As seen in Figure 2, four vibrational levels exist below the classical potential energy barrier in the double well. These levels appear grouped in two pairs of nearly degenerate vibrational states, the splitting of the lower pair being clearly smaller than the one corresponding to the higher pair (see Table 5). The probability density function of the ground state (and the one corresponding to the almost degenerate second state) is concentrated around the minima, becoming nearly zero at the transition state region. As a consequence, the proton is not centralized and system **2** contains a normal hydrogen bond. The chemical shift $\langle\delta\rangle_1$ is also normal for a hydrogen bond, only slightly more than the δ value corresponding to the frozen minima structure but much less than the δ value of the transition state structure (see Table 4). The evolution of $\langle\delta\rangle_i$ when going up along the series of vibrational levels is quite interesting. It is not monotonic at all: $\langle\delta\rangle_2$ turns out to be somewhat smaller than $\langle\delta\rangle_1$ because, although the $|\Psi|^2$ of the two first states almost vanishes at the central region (no difference is seen at the scale of Figure 2), only the wave function of the second state has strictly a node at the transition state structure (just at the middle of the hydrogen bond). Conversely, $\langle\delta\rangle_3$ is quite high because in the third level $|\Psi_3|^2$ has an important contribution near (and, in part, at) the transition state region. On the contrary, the central node of the fourth-state wave function leads to a diminution of the chemical shift. Not surprisingly, the fifth state (the first above the energy barrier) concentrates $|\Psi_5|^2$ at the central region, leading to the maximum chemical shift along the series of states. As a matter of fact, and apart from the differences coming from the number of nodes, this state in hydrogen oxalate is analogous to the ground state in the XDK model (which is already above its energy barrier). In following up, the chemical shift decreases noticeably because of the back-migration of $|\Psi|^2$ toward the minima and beyond (a similar behavior was described above for the XDK model). This decrease is not monotonic either because of the central node of the even vibrational states, which appears because their corresponding wave functions are antisymmetric. The existence of that node has a noticeable effect in the vibrational states of hydrogen oxalate because of the huge values of δ at the transition state region in contrast with the comparatively low values at the minima regions. The appearance of those nodes has little effect in the case of the XDK model, where the difference between those two regions is very small.

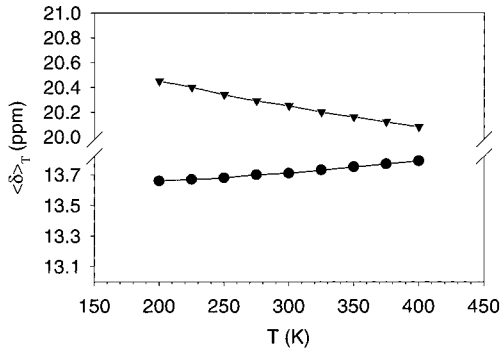

Figure 3. Proton NMR chemical shifts of the XDK model (triangles) and hydrogen oxalate (circles) as a function of the temperature.

So far we have shown that the evolution of the chemical shift along the series of vibrational states in an LBHB differs from that in a normal hydrogen bond. How could these differences be used to experimentally classify a hydrogen bond as an LBHB or a normal bond? At first glance, the measurement of the chemical shift for a set of vibrational states might enable us to distinguish between the two types of hydrogen bonds. If the vibrational states were very long-lived, distinct NMR spectra would be observed for each one. However, the transition rate from one vibrational state to another is expected to be quite fast in comparison with the NMR time scale, so that, as mentioned above, the observed chemical shift will be a Boltzmann weighted average over the thermally accessible states. Although the differences between an LBHB and a normal hydrogen bond are somewhat damped when the contributions of the vibrational states are mixed according to their population at thermal equilibrium, they are still significant. The dependence on the temperature of the $\langle\delta\rangle_T$ values for the XDK model and hydrogen oxalate is displayed in Figure 3. Although the slopes of both curves are quite small, the opposite trends are very clear. As temperature increases, the NMR chemical shift of the proton forming the hydrogen bond decreases in the XDK model (an LBHB) and increases in hydrogen oxalate (a normal hydrogen bond). However, these results have been obtained for a gas-phase model where no effects attributable to solvent or counterions have to be taken into account. Consequently, the different behavior of chemical shift with temperature

in our XDK model (an LBHB) and hydrogen oxalate, which is a normal hydrogen bond, reflects a property inherent to the LBHB in the gas phase. On the other hand, other effects do exist in solution that may also affect the behavior of the chemical shift of the transferring proton with temperature, for instance, the exchange of the LBHB proton with triethylamine (or with solvent molecules in general),[13] the nonequilibrium solvation effects, or the effect of the counterion.[29] Additional work (both experimental and theoretical) would be required to clarify the influence of those effects.

On a different subject, our theoretical results on the XDK model satisfactorily reproduce the absolute values of the experimental chemical shift in hexabenzyloxymethyl-XDK monoanion (19.2 and 18.0 ppm at −70 and 25 °C, respectively) obtained in apolar organic media with the corresponding counterion, despite the degree of modelization introduced in our system, thereby validating the goodness of the model used. Anyway, it would be unrealistic to expect quantitative agreement with experiment. Additionally, the theoretical values found in this paper for hydrogen oxalate agree satisfactorily with the experimental values of 14.0 and 15.6 ppm for ammonium hydrogen oxalate hemihydrate obtained by NMR spectroscopy in the solid state.[49,50]

Conclusions

In this paper we have theoretically studied the NMR chemical shift of the proton participating in the intramolecular hydrogen bond in both hexabenzyloxymethyl-XDK monoanion and hydrogen oxalate as a function of the temperature. To this aim, we used ab initio and DFT electronic calculations along with a monodimensional approach to solve the corresponding nuclear Schrödinger equation. Since the hexabenzyloxymethyl-XDK monoanion is quite large, we used a somewhat reduced system to model it.

The classical potential energy curve associated with the hydrogen bond in the hexabenzyloxymethyl-XDK monoanion has a double well shape with two very shallow minima on both sides of the proton transfer. The ground vibrational state appears to be slightly above the classical energy barrier, and the corresponding probability density function reaches its maximum value just at the transition state region, in such a way that the proton is localized at the center. Thus, in good agreement with previous experimental assumptions, the hydrogen bond in the hexabenzyloxymethyl-XDK monoanion turns out to be an LBHB.[28] Conversely, hydrogen oxalate contains a normal hydrogen bond, where the ground vibrational state is clearly below the energy barrier and the proton lies around the minimum energy structures.

The evolution of the proton NMR chemical shift along the series of vibrational levels is different in each case. In the hexabenzyloxymethyl-XDK monoanion, the higher the vibrational state, the smaller the corresponding chemical shift. In hydrogen oxalate, however, going up along the series of vibrational states the chemical shift tends to increase up to the first vibrational state above the energy barrier. These trends in hydrogen oxalate are not monotonic, given the existence of a central node in the even vibrational states. Since an NMR experiment at a given temperature measures the proton chemical shift of the species as a Boltzmann average of the chemical shifts associated with each vibrational level, a distinct dependence on the temperature can be expected in each case. In effect, as temperature increases, the thermally averaged NMR chemical shift of the proton joining the hydrogen bond in the hexabenzyloxymethyl-XDK monoanion decreases, in qualitative good agreement with experimental findings, whereas it increases in hydrogen oxalate.

The above-mentioned trends essentially depend on the features of the proton transfer double well and its corresponding vibrational wave functions. Therefore, opposite dependence on the temperature is expected to be a clear way to classify a hydrogen bond as an LBHB or a normal one. We note that, thus far, this conclusion is limited to hydrogen bonds in gas-phase symmetric potentials. It would be very interesting to extend the study of the dependence of the proton NMR chemical shift on the temperature to asymmetric potentials, including solvent and counterion effects. Additional work is currently underway on this subject in our laboratory.

To summarize, we must emphasize that, because some normal hydrogen bonds can involve large chemical shifts, the appearance of an unusually downfield proton NMR chemical shift is not conclusive evidence of the existence of an LBHB.[20,22,30] Consequently and taking into account the results presented in this paper, we propose that the dependence on the temperature of the NMR chemical shift for the proton forming the hydrogen bond in a symmetric potential can be used as a parameter to identify an LBHB in gas phase and possibly in inert solvents: A negative slope of the chemical shift as a function of the temperature is the fingerprint of an LBHB, whereas a positive slope announces a normal hydrogen bond.

Finally, we remark that the features of the LBHBs discussed in this paper have nothing to do with their proposed role in enzyme catalysis.

Acknowledgment. Financial support from DGES through Project No. PB95-0637 and the use of the Computational facilities of the "Centre de Computació i de Comunicacions de Catalunya" are gratefully acknowledged.

JA9742141

(49) Jeffrey, G. A.; Yeon, Y. *Acta Crystallogr.* **1986**, *B42*, 410.

(50) Zheng, L.; Fishbein, K. W.; Griffin, R. G.; Herzfeld, J. *J. Am. Chem. Soc.* **1993**, *115*, 5, 6254.